TU Delft

Delft University of Technology

Document Version
Final published version

Licence
CC BY-NC

Citation (APA)
Hu, Z., Temmerman, S., Wei, W., Liu, Z., Qiu, X., Xiong, L., Stive, M., Phan, K. L., Schuerch, M., Zhao, Z., Bouma, T. J., & Suzuki, T. (2026). Mangrove forests as natural protection from record-high storm waves. *Climate Risk Management*, *54*, Article 100874. https://doi.org/10.1016/j.crm.2026.100874

Important note
To cite this publication, please use the final published version (if applicable).
Please check the document version above.

Copyright
In case the licence states “Dutch Copyright Act (Article 25fa)”, this publication was made available Green Open Access via the TU Delft Institutional Repository pursuant to Dutch Copyright Act (Article 25fa, the Taverne amendment). This provision does not affect copyright ownership.
Unless copyright is transferred by contract or statute, it remains with the copyright holder.

Sharing and reuse
Other than for strictly personal use, it is not permitted to download, forward or distribute the text or part of it, without the consent of the author(s) and/or copyright holder(s), unless the work is under an open content license such as Creative Commons.

Takedown policy
Please contact us and provide details if you believe this document breaches copyrights.
We will remove access to the work immediately and investigate your claim.

This work is downloaded from Delft University of Technology.

Climate Risk Management 54 (2026) 100874

Contents lists available at ScienceDirect

Climate Risk Management

journal homepage: www.elsevier.com/locate/crm

Mangrove forests as natural protection from record-high storm waves

Zhan Hu [a,b,c], Stijn Temmerman [d], Wen Wei [e,*], Zezheng Liu [a,b,c], Xiufang Qiu [e], Lanlan Xiong [f], Marcel Stive [g], Khanh Linh Phan [h], Mark Schuerch [i], Zhiyuan Zhao [j], Tjeerd J. Bouma [j,k], Tomohiro Suzuki [l]

[a] School of Marine Sciences, Sun Yat-Sen University and Southern Marine Science and Engineering Guangdong Laboratory (Zhuhai), Zhuhai 519082, China
[b] State Key Laboratory of Environmental Adaptability for Industrial Products, Sun Yat-sen University, Zhuhai, China
[c] Guangdong Provincial Key Laboratory of Marine Resources and Coastal Engineering, Guangzhou, China
[d] Ecosphere Research Group, University of Antwerp, Antwerp, Belgium
[e] Guangdong Provincial Key Laboratory of Information Technology for Deep Water Acoustics, School of Ocean Engineering and Technology, Sun Yat-sen University, Guangzhou, China
[f] Guangdong Center for Marine Development Research, Guangzhou, China
[g] Hydraulic Department, Faculty of Civil Engineering and Geosciences, Delft University of Technology, the Netherlands
[h] Hydraulic Department, Faculty of Civil Engineering, Thuy Loi University, Viet Nam
[i] Department of Geography, Catchments and Coasts Research Group, University of Lincoln, United Kingdom
[j] Department of Estuarine and Delta Systems, NIOZ Royal Netherlands Institute for Sea Research, Utrecht University, Yerseke, the Netherlands
[k] Department of Physical Geography, Faculty of Geosciences, Utrecht University, Utrecht, the Netherlands
[l] Department of Civil Engineering, KU Leuven, Leuven, Belgium

ARTICLE INFO

Keywords:
Mangroves
Nature-based solution
Coastal protection
Storm waves
Wave attenuation
Web-application

ABSTRACT

Coastal regions worldwide face growing flood risks from climate change. As the dominant coastal ecosystem in (sub)tropical zones, mangroves serve as natural buffers, mitigating wave action and reducing flood hazards. However, field evidence of their efficacy during extreme storm events remains scarce, limiting accurate estimation of their protective capacity. Here, we present unique measurements of storm waves (significant wave height up to 0.88 m) and their substantial attenuation (59%) within a mangrove forest, providing critical evidence that mangroves sustain significant wave attenuation capacity under extreme conditions. Utilizing this dataset, we demonstrate that a new predictive method outperforms traditional approaches in predicting wave evolution across mangroves. We have translated this advance into a user-friendly web application, enabling non-specialists to predict storm wave attenuation using available fair-weather field data. These findings confirm mangroves as essential nature-based protection against climate-intensified storm waves and provide a practical tool to advise on this protection.

1. Introduction

Mangrove wetlands are among the most vital ecosystems fringing (sub) tropical coastlines worldwide. They act as natural buffers

* Corresponding author.
E-mail address: weiw95@mail.sysu.edu.cn (W. Wei).

https://doi.org/10.1016/j.crm.2026.100874
Received 9 December 2025; Received in revised form 16 August 2026; Accepted 20 August 2026
Available online 21 August 2026
2212-0963/© 2026 The Authors. Published by Elsevier B.V. This is an open access article under the CC BY-NC license (http://creativecommons.org/licenses/by-nc/4.0/).

that protect hinterlands and coastal communities from storm-induced flooding and erosion by dissipating wave energy and promoting sediment accretion, thereby keeping pace with long-term sea-level rise (Temmerman et al., 2023; Huang et al., 2026). Beyond their physical protection function, mangroves deliver numerous ecosystem services, such as sustaining fisheries, sequestering carbon, and improving water quality (Dahdouh-Guebas et al., 2022). These multifaceted benefits render mangrove conservation and restoration particularly crucial for developing, low-latitude nations, where socioeconomic vulnerability to coastal hazards is often acute.

Mangroves attenuate wave energy primarily through drag forces generated by their complex aerial structures (canopy, trunk, and aboveground root systems), with efficiency governed by the interplay of vegetation properties (e.g., plant density, stem/root diameters, and canopy properties) and ambient hydrodynamic conditions (e.g., wave height, water depth) (Horstman et al., 2014; Hu et al., 2025). In numerical modeling, this biophysical interplay is commonly parameterized using a bulk drag coefficient (C_D) (Dalrymple et al., 1984; Mullarney et al., 2017; Lopez-Arias et al., 2024). However, C_D exhibits substantial dynamic variability even for a specific mangrove forest, due to variations in flow conditions and vegetative reconfiguration (Yoshikai et al., 2022; Temmerman et al., 2023). The absence of a consensus on its parameterization introduces significant uncertainty into wave attenuation predictions, consequently limiting the reliable assessment of mangrove protective capacity across diverse coastal environments.

Despite the growing acknowledgment of mangrove coastal protection value, in situ measurements of wave propagation and transformation remain remarkably scarce (Fig. 1). This scarcity leads to uncertainties in quantifying and applying wave attenuation capacity. Existing field studies are predominantly clustered in a few regions, such as southern China (e.g., Zhou et al., 2022; Huang et al., 2024), Vietnam (e.g., Nguyen et al., 2017; Norris et al., 2017), northern coast of South America (e.g., Sánchez-Núñez et al., 2020; Best et al., 2022), and Australia (e.g., Lopez-Arias et al., 2024) (see also Fig. 1 and Table S1). In contrast, vast stretches of the world's mangrove coastlines, including the entire African coast and much of Southeast Asia, lack documented wave measurements to our knowledge. Furthermore, most existing wave measurements in mangroves have been conducted under non-storm or mild conditions, with incident significant wave heights (H_s) typically below 0.5 m (Fig. 1b). As a result, the wave attenuation capacity of mangroves during extreme storm events—when their protective role is most critical—remains poorly quantified. This critical lack of high-energy data raises a fundamental question: can existing empirical and semi-empirical models reliably predict the capacity of mangroves to attenuate extreme storm waves?

Addressing this knowledge gap is vital for scaling up mangrove-based coastal protection strategies. In the current study, we address this gap by: *i*) conducting in situ measurements of wave attenuation within mangroves under real storm conditions; *ii*) using these observations to validate and recalibrate predictive models for high-energy regimes; and *iii*) developing an accessible, intuitive platform that enables local practitioners to evaluate the wave attenuation capacity of their mangrove systems during extreme events. With newly acquired record-high wave observations and a newly developed field-calibrated predictive framework of Hu et al. (2025) (the *HU* method; see details in section 2.3), our research addresses all three priorities. These contributions narrow key gaps in the global understanding of mangrove–wave interactions and enhance the capacity to implement mangrove forests as effective, nature-based coastal defenses against intensifying storms.

The paper is organized as follows: Section 2 describes the field measurements and the wave prediction methods; Section 3 presents the record-high wave observations and their attenuation; Section 4 compares the *HU* method with drag-based models; Section 5 introduces the web application and its practical use; Section 6 concludes the study.

2. Materials and methods

2.1. Compiling data of top incident wave height

To compile the global incident wave height (H_{s0}) dataset shown in Fig. 1, we conducted a comprehensive literature survey using the Web of Science Core Collection (1900–2025) in May 2025. The search query—Topic = (wave attenuation) AND (mangrove OR typhoon)—yielded 364 articles. Among them, 17 studies directly reported field-measured H_{s0} data, while an additional 25 articles were identified as review papers summarizing related findings. We further examined the bibliographies of these review papers and identified four more studies with explicit H_{s0} measurements. In total, 21 peer-reviewed publications providing quantitative H_{s0} data were incorporated into the global compilation (see also Table S1). This dataset provides the first near-global comparison of wave conditions across mangrove ecosystems, highlighting the rarity of storm-wave observations (Fig. 1b).

2.2. Wave observation under normal and typhoon conditions

Between 2 and 8 September 2024, Super Typhoon Yagi swept across the Philippines and southern China (Fig. 2a), ranking among the most intense typhoons ever documented in northern Vietnam and the South China Sea (Van Dijk et al., 2025). During its landfall near Zhanjiang City, South China, on 6 September 2024, the storm generated sustained winds exceeding 210 km h^{-1}, producing exceptionally energetic waves that impacted our observation site.

Our in situ wave measurements were carried out across a restored mangrove wetland along the Zhanjiang Coast, South China, covering two contrasting hydrodynamic periods: (i) August 8–September 11, 2024, which captured the passage of Super Typhoon Yagi, and (ii) March 2–May 6, 2025, representing calm-weather conditions (Fig. 2a and b). Three RBRsolo^3 pressure sensors were deployed along a cross-shore transect extending from the bare tidal flat into a mature *Avicennia marina* mangrove forest (Fig. S1). Vegetation surveys along the transect (3 m × 3 m quadrats) showed that the mature zone (131–250 m from the seaward edge) has an average stem density of 6 stems/m^2, mean stem diameter of 0.0425 m, and canopy height of 4 m; The pioneer zone (100–130 m) has reduced canopy height (1.5 m) and stem density (2.28 stems/m^2). The measurement transect was positioned perpendicular to the

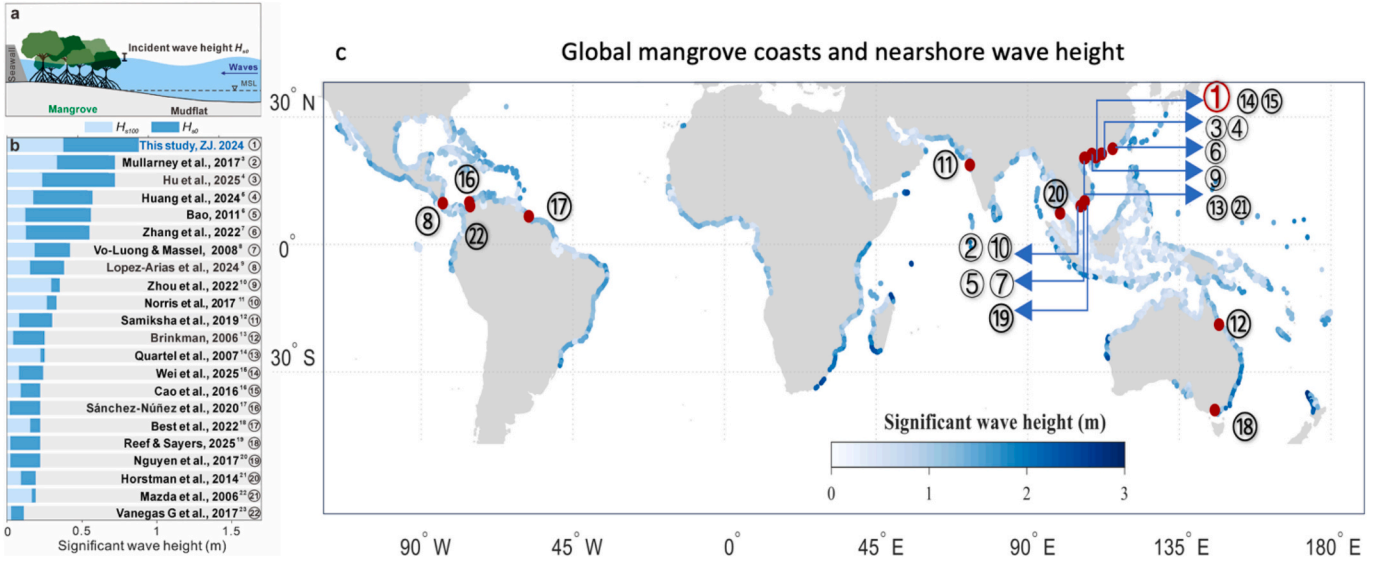


Fig. 1. Reported wave measurements in mangroves at a global scale. (a) Conceptual diagram of mangrove wetlands as nature-based solutions, and the definition of H_{s0} as the incident significant wave height at mangrove seaward edge. (**b**) Reported H_{s0} and H_{s100} as residual wave height after 100 m propagation in mangrove forest (Text S1) (Brinkman, 2006; Mazda et al., 2006; Quartel et al., 2007; Vo-Luong and Massel, 2008; Quang Bao, 2011; Horstman et al., 2014; Cao et al., 2016; Mullarney et al., 2017; Nguyen et al., 2017; Norris et al., 2017; Samiksha et al., 2019; Vanegas G et al., 2019; Sánchez-Núñez et al., 2020; Best et al., 2022; Zhang et al., 2022; Zhou et al., 2022; Huang et al., 2024; Lopez-Arias et al., 2024; Reef and Sayers, 2025; Wei et al., 2025; Hu et al., 2025). The highest H_{s0} is 0.88 m, measured at Zhangjiang coast (ZJ) in 2024 from the current study. (**c**) Global distribution of mangrove coasts, their corresponding nearshore wave height and the site of wave measurements. The shown nearshore wave height is the 80th percentile value of annual significant wave height from the ERA5 reanalysis as a representative for storm conditions (Hersbach et al., 2020).

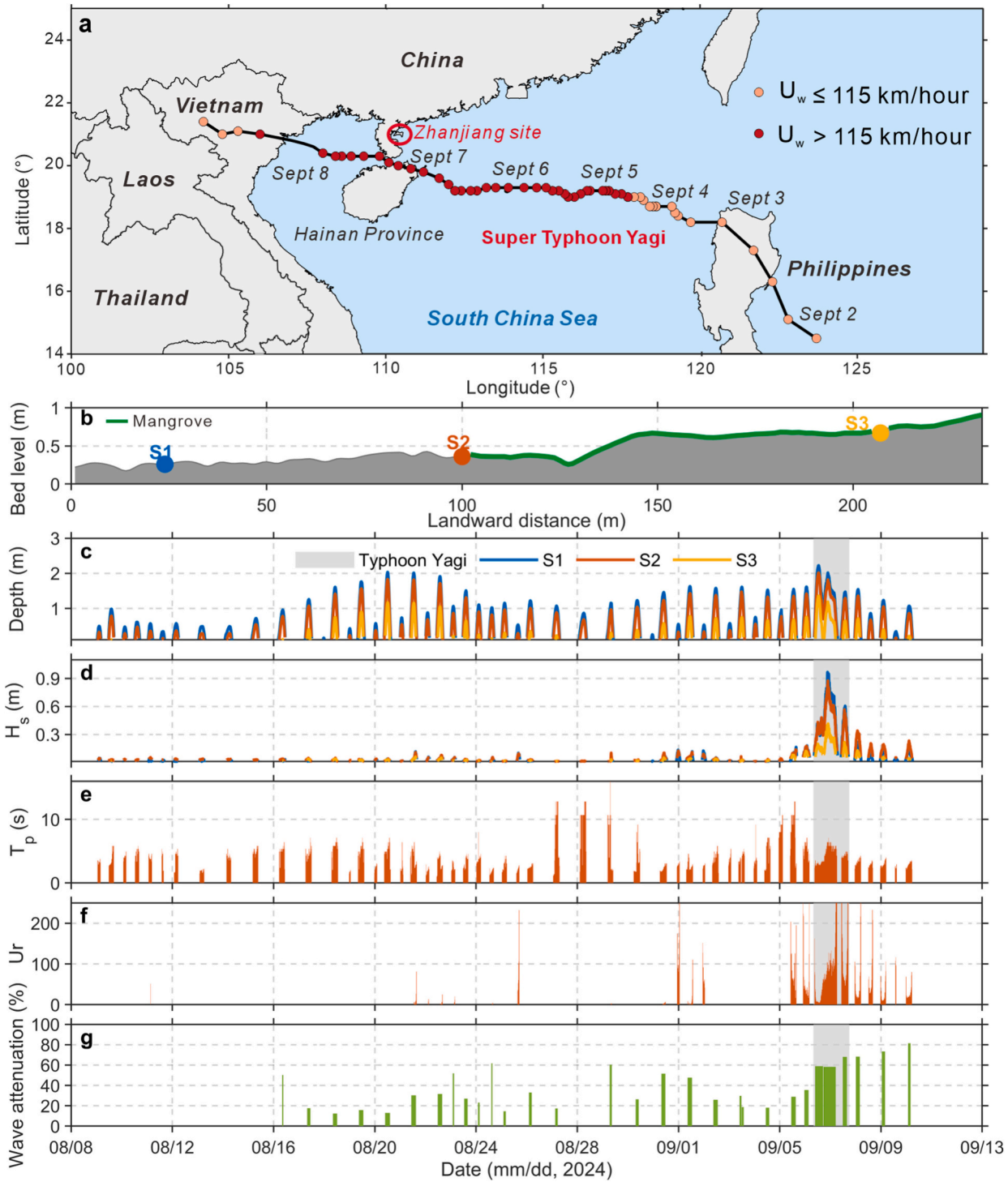


Fig. 2. Observations during the Typhoon Yagi. **(a)** track of Super Typhoon Yagi (data from http://typhoon.nmc.cn/), and our measurement site (110°10′13.61″E, 20°55′33.12″N) at Zhanjiang coast. **(b)** Bathymetric profile (with the mangrove zone labeled as a thick green line) and wave observational stations. **(c)** water depth, **(d)** significant wave height, **(e)** peak wave period at the station S2, **(f)** *Ur* number at S2, and **(g)** wave attenuation between the stations S2 and S3 at the Zhanjiang Mangrove Site. S1 is the most seaward measuring station and S2 is the one at the mangrove forest edge. The measurements were conducted from Aug 8 to Sep 13, 2024, and Typhoon Yagi passage was during Sep 6–8. (For interpretation of the references to colour in this figure legend, the reader is referred to the web version of this article.)

seaward mangrove edge, in an area representing the mean mangrove stem density, diameter and canopy height. All instruments withstood the storm, yielding one of the first continuous, high-fidelity wave records across a mangrove forest during a super typhoon. Each sensor had a measurement range of 20 dbar, with a resolution of 0.001% and accuracy of ±0.05%. Sensors continuously recorded pressure at 4 Hz with a 10-min sampling interval, providing high-frequency, long-term time series across tidal cycles and storm conditions. The recorded pressure data were processed to derive significant wave height (H_s), peak wave period (Tp), and instantaneous water depth (h) following standard spectral analysis procedures (Tucker and Pitt, 2001). Bathymetry along the transect was surveyed using RTK-GPS at 2 m intervals, referenced to the mean low water level (MLWL). The survey data were interpolated to obtain a continuous bathymetry (Fig. 2b). The measured hydrodynamic and bathymetric data were included in a repository dataset (Hu and Zhao, 2025).

2.3. Prediction of wave evolution across mangroves

To evaluate the accuracy and applicability of existing wave attenuation prediction approaches under extreme conditions, we compared three representative methods (Table S2). The first two are widely used drag-based models: a classical analytical model (Dalrymple et al., 1984) and the non-hydrostatic numerical model SWASH (Suzuki et al., 2019). Both approaches simulate wave propagation by resolving the drag force exerted by mangrove stems and roots on oscillatory flow. As such, their predictive performance depends critically on the selection of drag coefficients (C_D), which must be prescribed a priori based on empirical or laboratory-derived relations. Ten established C_D formulations from the literature were incorporated to ensure comprehensive evaluation (Table S3). These formulations vary in their parameterization of vegetation geometry, Reynolds number dependence, and flow regimes, thus yielding a range of plausible C_D values for model input.

The third method is the newly developed *HU* method, a non-drag-based predictive framework (Hu et al., 2025). Unlike conventional models that rely on explicit drag parameterization, the *HU* method was built upon H_{Ln}-Ur relations, where H_{Ln} is relative wave height (ratio between in-canopy and incident wave height) over n wavelengths and Ur is the *Ursell* number ($= H_{s0}\,L^2/D^3$, where L is wavelength and D is water depth at the seaward edge of the canopy), a common metric for wave nonlinearity (Phan et al., 2019). At each wavelength, a general form of the H_{Ln}-Ur relation is as follows:

$$H_{Ln} = 1/\left(1 + a \cdot Ur^b\right) \tag{1}$$

where a and b (varying with n) are calibrated from low-wave measurements. The core premise is that larger wave nonlinearity (higher U_r) enhances energy dissipation within vegetation, leading to lower H_{Ln} values. For any given Ur, H_{Ln} can be iteratively determined along the transect as the cumulative number of wavelengths increases (Fig. 3b), thereby quantifying the progressive, distance-dependent wave attenuation induced by the mangroves. For a given wave burst, L is held constant along the transect. This simplification is justified because the transect is short (~100 m) and the bed slope is mild, so depth variations are limited.

The second field campaign (March–May 2025) provided calm-weather measurements ($H_{s0} < 0.4$ m), which were subsequently used to predict storm-wave attenuation during Typhoon Yagi (when $H_{s0} > 0.5$ m) to test the generalization of major predictive methods from calm-condition observations to high-energy waves. Model comparison between the three types of models was conducted using all valid bursts of low incident waves ($H_{s0} < 0.5$ m) and high incident waves ($H_{s0} > 0.5$ m). For the *HU* method, both low- and high-wave predictions were based on calm-weather calibration (low-wave data used to derive H_{Ln}-Ur relations, which were then applied to high waves). For the drag-based models, predictions were made directly using ten pre-determined C_D relations (Table S3), with Reynolds numbers and Keulegan-Carpenter numbers to determine C_D calculated from our observed waves and vegetation parameters. The coefficient of determination ($R^2 = 1 - sum\left(y_i - f_i\right)^2 / sum\left(y_i - \bar{y}\right)^2$, where y_i and f_i are measured and predicted wave height, respectively, and $\bar{y}$ is the mean measured wave height) and root mean square error (*RMSE*) were then calculated between predicted and observed wave heights for both low and high wave cases. Notably, negative R^2 values could occur, indicating poor generalization of the models, whose predictions are worse than simply using the mean of the observed wave heights.

3. Record-high incident wave in mangroves

Under normal conditions at the Zhanjiang site, incident significant wave heights (H_{s0}) are below 0.10 m, with peak wave periods of 2.0–10.0 s and a maximum water depth of 2 m (Fig. 2). The extreme waves during Typhoon Yagi (September 6–8) are clearly extreme values in the dataset (Fig. 2), with H_{s0} mostly exceeding 0.5 m and wave periods of 4.0–6.4 s, with a maximum water depth of 1.82 m. Notably, our observation captured an extreme H_{s0} of 0.88 m at the *Avicennia marina* mangrove front (Station S2), establishing a new global record for in situ mangrove wave records and exceeding the previously reported maximum by approximately 22% (Fig. 1b). As a comparison, the H_{s0} measured during the calm period (Mar–May 2025) is 0.05–0.22 m, with wave periods of 2–6 s and a maximum water depth of 1.57 m during spring tide (Fig. S2).

The measurements demonstrate that even under super typhoon conditions, the mangrove forest maintained a remarkable capacity to attenuate incident wave energy (Fig. 1b). The peak $H_{s0} = 0.88$ m at the mangrove front was attenuated to 0.36 m across a 100 m-long vegetated transect, corresponding to a 59% reduction in wave height (Fig. 2). Across all high-energy events ($H_{s0} > 0.5$ m; 59 bursts during September 6–8), wave attenuation ranged from 44% to 70%, consistent with or exceeding attenuation rates reported under non-storm or moderate wave conditions (13–52% for 70 bursts during August 20–23 and 1–50% for 87 bursts during April 1–3, both $H_{s0} <$ 0.5 m).

Critically, post-storm surveys revealed no large-scale structural damage to the mangrove stand (Fig. S1), with only minor

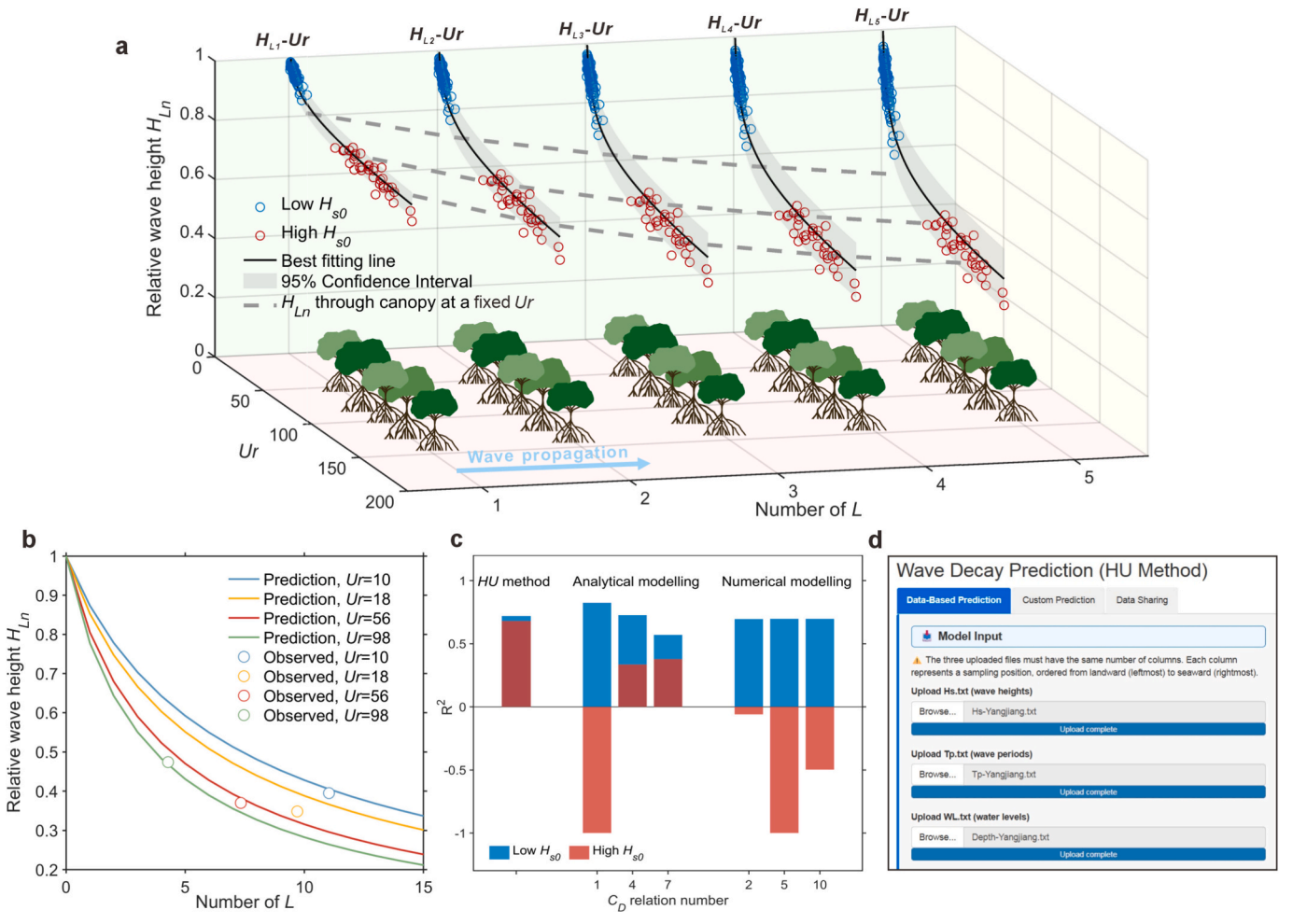


Fig. 3. Prediction of wave reduction in storm conditions using a web-application based on the *HU* method. **(a)** Relations of H_{Ln} and Ursell number (*Ur*) at 1–5 wavelengths (*L*) in the mangrove forest, as an illustration of the *HU* method. At each number of wavelengths, a fitted H_{Ln}-*Ur* curve can be derived based on low H_{s0} cases (0.1 m < H_{s0} < 0.4 m). The data points of high H_{s0} cases also fall on these curves. Subsequently, for a given *Ur* number, the evaluation of H_{Ln} along the mangrove (as the number of *L* increases, dashed lines) can be obtained for both low and high H_{s0} cases. The dashed lines are translated into the 2D representation in panel **(b)**, where each line corresponds to a fixed *Ur* value. (**b**) Examples of predicted and observed relative wave height with a sequence of *L* with given *Ur* numbers. (**c**) Performance of the three different methods (measured by R^2 values) in predicting wave attenuation. For the two methods based on C_D relations (analytical and numerical modeling), we show the selected top 3 C_D relations that result in highest R^2 values in high H_{s0} cases. For visual clarity, R^2 values below −1 are plotted as −1. A complete summary of the model performance is shown in Table S4. (**d**) Interface of the web-application based on the *HU* method (see Method section and Text S1) (Zhao et al., 2025).

defoliation or uprooting of fringe trees. Throughout the typhoon event, wave attenuation across the mangrove remained high, with no systematic decline post the event (73%–81% after September 9) (Fig. 2g). The integrity of the majority of the vegetation, combined with the sustained wave attenuation, indicates an intrinsic adaptive capacity of mangroves to withstand and mitigate storm waves without systemic collapse. These findings provide the first empirical confirmation that mangroves can effectively mitigate wave energy during super typhoon conditions, reinforcing their role as resilient, nature-based coastal defenses. Consequently, this unique dataset serves as a crucial benchmark for calibrating predictive models and for evaluating wave attenuation by coastal wetlands under extreme wave forcing.

4. Predictions of storm wave attenuation by mangroves

For the conventional drag-based models, the ten empirical C_D relations (Table S3) were applied using the vegetation parameters of the mature mangrove zone (see Section 2.2). The pioneer zone was not explicitly resolved because it is narrow (30 m) and could contribute little to the overall wave attenuation. These parameters were used to compute Reynolds numbers and Keulegan-Carpenter numbers from the observed wave data to determine the C_D values for each relation (Table S3), and also to model wave attenuation. The determined C_D values ranged from 0.35 to 2.47 under high-wave conditions at our site, with substantial variation among relations. The resulting spread in C_D-based predictions is shown in Fig. S3 and summarised by the R^2 and *RMSE* values in Table S4.

In contrast, the *HU* method is data-driven and does not require explicit parameterization of individual vegetation zones, as spatial heterogeneity is automatically accounted for through calibration with measured wave heights. The method was calibrated using low-wave data, yielding calibration parameters a and b in Eq. (1) ranging from 0.0157 to 0.4420 and 0.5650 to 0.6449, respectively, depending on the wavelength number n (Fig. 3a). Using these relations, the relative wave height H_{Ln} decreases progressively with increasing n for a given Ur (Fig. 3b). Notably, the fitted H_{Ln}-Ur lines become progressively steeper as the number of wavelengths through the canopy increases, reflecting cumulative energy dissipation with distance (Fig. 3a and b).

The performance test of these three methods further demonstrates that the *HU* method delivers more accurate predictions of wave attenuation under the record-breaking storm waves of Typhoon Yagi than the two drag-based models. For high incident wave heights ($H_{s0} > 0.5$ m), the *HU* method achieved an R^2 of 0.68 and an *RMSE* of 0.04 m, substantially outperforming the average of the C_D-based models (with maximum R^2 values 0.38 for the theoretical model and − 0.06 for SWASH; see Fig. 3c and Table S4). This is further illustrated in Fig. S3, where the *HU* method's predicted attenuation closely matches field observations, while most C_D-based predictions show large deviations. Such a performance is notable as it was attained using low-energy calibration data collected six months apart from the typhoon. If the wave data near the typhoon event were applied in the *HU* method, the R^2 can be increased to 0.75, showing consistent high accuracy. In contrast, both drag-based models, regardless of complexity, accurately predicted attenuation only under low-energy conditions (with a mean R^2 of 0.51; Table S4), where the *HU* method still exhibited higher accuracy ($R^2 = 0.87$; Table S4). The reduced performance of drag-based methods in high wave cases (Fig. S3, Table S4) indicates poor generalization of these models from calm conditions to high-wave conditions. These results highlight the higher accuracy of *HU* method over the traditional drag-based methods.

The key advantage of the *HU* method is that it avoids the parametric uncertainty of drag-based models under high-energy conditions where vegetation reconfiguration and turbulent flows prevail. Specifically, this method does not explicitly model drag or reconfiguration. Instead, it relies on the calibrated H_{Ln}-Ur relations, where Ur integrates wave nonlinearity and implicitly captures bulk dissipation. As long as the range of Ur during storms does not exceed that in low-wave conditions (since Ur depends strongly on water depth and period, not only on wave height; see Fig. 2f), the method is reliable.

While the *HU* method-based application demonstrates robust performance in predicting storm wave attenuation from calm-weather data, several limitations should be noted. It requires two wave stations along a transect to derive the H_{Ln}-Ur relations, and prior field campaigns are necessary to generate them. Secondly, our validation covers H_{s0} up to 0.88 m, while more extreme conditions when vegetation reconfiguration prevails remain untested. Lastly, the *HU* method performs best where bed slopes are mild and gradual and depth-limited breaking is minimal. Under such conditions, wave attenuation is dominated by vegetation drag, while interference from other factors (e.g., bed friction, wave breaking, abrupt bathymetric changes) remains small. This ensures that the empirically derived H_{Ln}-Ur relations primarily reflect vegetation-induced dissipation, leading to more robust predictions when extrapolating to storm conditions. The bathymetric influence on the performance is not clear. Addressing these limitations and isolating the influencing processes will further enhance the generalizability of the *HU* method.

5. An intuitive web-application for predicting storm wave attenuation

Building upon the successful validation of the *HU method* using the highest in situ wave measurements ever recorded in mangrove environments, we developed an interactive web-based application (https://nioz.shinyapps.io/Wave-Decay-Prediction-HU-Method/; Zhao et al., 2025) to allow non-specialists to predict storm wave attenuation by mangroves (Fig. 3). The accompanying web-application, implemented in R language, allows users to upload local wave datasets to automatically compute and visualize attenuation performance under storm conditions (Fig. 2d). The platform provides freely downloadable results and supports real-time assessment of mangrove-based wave attenuation (Zhao et al., 2025). Additional details on the computational algorithms, web-application architecture, and the analytical/numerical wave models are provided in the Supplementary Information (Text S1).

This web application enables wave attenuation assessment in mangrove forests under storm conditions without the need for complex numerical modeling. It features three core interfaces: **(a) Data-based Prediction:** Users can upload field-measured wave data to automatically calibrate the model and predict wave attenuation under storm scenarios. **(b) Custom Prediction:** Allows manual

entry or batch upload of storm parameters (e.g., wave height, period, depth, and vegetation width) for single or multiple scenario simulations. This allows practitioners to estimate the required mangrove width under the envisioned storm wave conditions in restoration projects. **(c) Data Sharing:** Serves as a collaborative platform for researchers and practitioners to contribute and access quality wave data, fostering evidence-based mangrove conservation and coastal resilience planning.

Traditionally, estimating vegetation-induced wave attenuation requires sophisticated analytical or numerical modeling, demanding specialized knowledge and extensive computational experience. In contrast, the new web-application is designed for coastal practitioners, conservation managers, and policymakers who may lack formal hydrodynamic modeling expertise. Through a simple upload interface, users can input locally measured hydrodynamic parameters, including water depth, peak wave period, and significant wave height obtained under calm-weather conditions, to generate quantitative predictions of mangrove-induced attenuation during extreme storm events. Notably, the tool is most appropriate as a decision-support product used together with specialists who have a basic understanding of wave dynamics and coastal processes. Interpretation of the predicted attenuation rates, particularly regarding data quality, prediction uncertainty, and site-specific limitations (Section 4), should be undertaken with appropriate expertise.

This approach fundamentally democratizes access to wave modeling tools and is particularly beneficial for developing and least-developed coastal nations, where nature-based coastal protection strategies are urgently needed but technical and financial resources remain limited (Edmonds et al., 2020). By offering a transparent, open-access computational platform, the web-application bridges the gap between cutting-edge coastal science and local-scale management practices.

In parallel, our global literature survey revealed a pronounced data scarcity in wave measurements across mangrove ecosystems, particularly in vulnerable and under-observed regions such as Africa, Southeast Asia, and Latin America. The web-application is therefore not merely a predictive tool, but also serves as a collaborative scientific platform. We encourage global users to contribute their wave measurements, particularly during storm events, to expand the empirical database of mangrove hydrodynamics. Such community-driven data sharing can substantially enhance both the validation and regional generalization of the *HU* method and advance a global understanding of mangrove-mediated wave attenuation under current and future wave climates (Morim et al., 2023).

Acknowledging the financial constraints of field instrumentation, we recommend several cost-efficient strategies: *i)* deploying a minimum of two sensors; *ii)* testing lower-cost sensors with sufficient accuracy for wave measurements (see e.g. Figurski et al., 2011); *iii)* partnering with local hydrological agencies to access wave sensors. Notably, the *HU* method is site- and transect-specific. For a different part of the same forest with different vegetation structure, or for a different forest altogether, new calibration measurements are necessary. If a forest suffers major damage during or before the storm, new relationships should be established using post damage measurements. Users should not blindly extrapolate the results across heterogeneous zones without validation.

We envision this tool as a catalyst for science-policy integration, empowering coastal communities to design and optimize mangrove-based protection projects through accessible, evidence-based modeling. We therefore recommend the adoption of this web-application as a decision-support tool for promoting mangrove restoration and sustainable coastal resilience worldwide. Through our web-application, we could collect cases for young, mature, and mixed-complexity mangrove forests. Guidance is then provided on estimating the required cross-shore width for a target residual wave height, on the influence of planting density (by scaling width), and on recalibration over time as forests mature. These additions enable practitioners to move beyond assessing existing protection to designing new nature-based solutions.

6. Conclusions

The current understanding of mangrove-induced wave attenuation during storm events is fundamentally limited by the scarcity of observational data under extreme conditions. Our research provides a critical advance by capturing in situ measurements during Super Typhoon Yagi, which observed record-high incident storm waves (up to 0.88 m). The results offer definitive empirical validation: a 59% reduction in wave height over 100 m of forest, confirming the significant role of mangroves in coastal defense even during a super typhoon. Furthermore, we operationalize this knowledge through a newly developed web application, engineered to be precise, accessible, and user-friendly. By democratizing predictive capabilities, this application is anticipated to foster the widespread integration of mangroves into coastal protection schemes and make a substantive contribution to global mangrove conservation efforts.

CRediT authorship contribution statement

Zhan Hu: Writing – original draft, Methodology, Conceptualization. **Stijn Temmerman:** Writing – review & editing, Formal analysis. **Wen Wei:** Funding acquisition, Conceptualization. **Zezheng Liu:** Writing – original draft, Formal analysis. **Xiufang Qiu:** Writing – original draft, Formal analysis. **Lanlan Xiong:** Funding acquisition. **Marcel Stive:** Writing – original draft, Formal analysis. **Khanh Linh Phan:** Writing – original draft, Formal analysis. **Mark Schuerch:** Writing – original draft, Data curation. **Zhiyuan Zhao:** Software. **Tjeerd J. Bouma:** Software. **Tomohiro Suzuki:** Writing – original draft, Data curation.

Declaration of competing interest

The authors declare that they have no known competing financial interests or personal relationships that could have appeared to influence the work reported in this paper.

Acknowledgments

We would like to thank the members of M5 Lab (Mudflat, Marsh, Mangrove, Measurement & Modeling) and Quan Xie at Sun Yat-sen University for the discussion and assistance in this work. This work is supported by Guangdong Basic and Applied Basic Research Foundation (2024B1515020066, 2024A1515010096), the National Natural Science Foundation of China (42176202, 42276173 and 12411530096), Guangxi Science and Technology Program (Grant No. FN2600640197), Innovation Group Project of Southern Marine Science and Engineering Guangdong Laboratory (Zhuhai) (311021004), and 111 Project (B21018).

Appendix A. Supplementary data

Supplementary data to this article can be found online at https://doi.org/10.1016/j.crm.2026.100874.

Data availability

https://doi.org/10.4121/ec93da24-1ecc-447f-ba53-1646c40b06de.v1

References

Best, Ü.S.N., van der Wegen, M., Dijkstra, J., Reyns, J., van Prooijen, B.C., Roelvink, D., 2022. Wave attenuation potential, sediment properties and mangrove growth dynamics data over Guyana's intertidal mudflats: assessing the potential of mangrove restoration works. Earth Syst. Sci. Data 14 (5), 2445–2462. https://doi.org/10.5194/essd-14-2445-2022.

Brinkman, R.M., 2006. Wave attenuation in mangrove forests: an investigation through field and theoretical studies [Phd, James Cook University]. Doi:. https://doi.org/10.25903/bhd9-na63.

Cao, H., Chen, Y., Tian, Y., Feng, W., 2016. Field investigation into wave attenuation in the mangrove environment of the South China Sea coast. J. Coast. Res. 32 (6), 1417–1427. https://doi.org/10.2112/JCOASTRES-D-15-00124.1.

Dahdouh-Guebas, F., Friess, D.A., Lovelock, C.E., Connolly, R.M., Feller, I.C., Rogers, K., Cannicci, S., 2022. Cross-cutting research themes for future mangrove forest research. Nat. Plants 8 (10), 1131–1135. https://doi.org/10.1038/s41477-022-01245-4.

Dalrymple, R.A., Kirby, J.T., Hwang, P.A., 1984. Wave diffraction due to areas of energy dissipation. J. Waterw. Port Coast. Ocean Eng. 110 (1), 67–79. https://doi.org/10.1061/(ASCE)0733-950X(1984)110:1(67).

Edmonds, D.A., Caldwell, R.L., Brondizio, E.S., Siani, S.M.O., 2020. Coastal flooding will disproportionately impact people on river deltas. Nat. Commun. 11 (1), 4741. https://doi.org/10.1038/s41467-020-18531-4.

Figurski, J.D., Malone, D., Lacy, J.R., Denny, M., 2011. An inexpensive instrument for measuring wave exposure and water velocity. Limnol. Oceanogr. Methods 9, 204–214.

Hersbach, H., Bell, B., Berrisford, P., Hirahara, S., Horányi, A., Muñoz-Sabater, J., Nicolas, J., Peubey, C., Radu, R., Schepers, D., Simmons, A., Soci, C., Abdalla, S., Abellan, X., Balsamo, G., Bechtold, P., Biavati, G., Bidlot, J., Bonavita, M., Thépaut, J.-N., 2020. The ERA5 global reanalysis. Q. J. R. Meteorol. Soc. 146 (730), 1999–2049. https://doi.org/10.1002/qj.3803.

Horstman, E.M., Dohmen-Janssen, C.M., Narra, P.M.F., van den Berg, N.J.F., Siemerink, M., Hulscher, S.J.M.H., 2014. Wave attenuation in mangroves: A quantitative approach to field observations. Coast. Eng. 94, 47–62. https://doi.org/10.1016/j.coastaleng.2014.08.005.

Hu, Z., Zhao, Z., 2025. Data and code to build a web-application for assessing nature-based attenuation of extreme waves by mangroves (dataset). https://data.4tu.nl/private_datasets/KXxcZbtCfhaXWdtdc9kxSs9T3O-Yx_PCh2ugj3aCy6M.

Hu, Z., Temmerman, S., Zhu, Q., Wang, X., Wu, J., Xu, T., Schoutens, K., Suzuki, T., Yang, Z., Bouma, T.J., 2025. Predicting nature-based coastal protection by mangroves under extreme waves. Proc. Natl. Acad. Sci. 122 (12), e2410883122. https://doi.org/10.1073/pnas.2410883122.

Huang, K., Hu, Z., Liu, Z., Paul, M., Xu, T., Suzuki, T., 2024. Pinpointing the role of wave period in vegetation induced wave attenuation. Coast. Eng. 193, 104568. https://doi.org/10.1016/j.coastaleng.2024.104568.

Huang, K., Schuerch, M., Fagherazzi, S., Liu, Z., Hu, Z., 2026. Climate change influences coastal protection value of global wetlands. Sci. Bull. 71, 2339–2347.

Lopez-Arias, F., Maza, M., Calleja, F., Govaere, G., Lara, J.L., 2024. Integrated drag coefficient formula for estimating the wave attenuation capacity of *Rhizophora* sp. mangrove forests. Front. Mar. Sci. 11. https://doi.org/10.3389/fmars.2024.1383368.

Mazda, Y., Magi, M., Ikeda, Y., Kurokawa, T., Asano, T., Mazda, Y., Magi, M., Ikeda, Y., Kurokawa, T., Asano, T., 2006. Wave reduction in a mangrove forest dominated by Sonneratia sp. Wetl. Ecol. Manag. 14 (4), 365–378. https://doi.org/10.1007/s11273-005-5388-0.

Morim, J., Wahl, T., Vitousek, S., Santamaria-Aguilar, S., Young, I., Hemer, M., 2023. Understanding uncertainties in contemporary and future extreme wave events for broad-scale impact and adaptation planning. Sci. Adv. 9 (2), eade3170. https://doi.org/10.1126/sciadv.ade3170.

Mullarney, J.C., Henderson, S.M., Reyns, J.A.H., Norris, B.K., Bryan, K.R., 2017. Spatially varying drag within a wave-exposed mangrove forest and on the adjacent tidal flat. Cont. Shelf Res. 147, 102–113. https://doi.org/10.1016/j.csr.2017.06.019.

Nguyen, L.T., Tri, V.P.D., Loi, L.T., Sasaki, J., Nobuoka, H., 2017. Assessment of the ability of mangrove structures for attenuation of coastal wave energy: A case study in Bac Lieu Province, Vietnam. . In Asian and Pacific Coasts 2017 (pp. 737–748).. WORLD SCIENTIFIC. https://doi.org/10.1142/9789813233812_0067.

Norris, B.K., Mullarney, J.C., Bryan, K.R., Henderson, S.M., 2017. The effect of pneumatophore density on turbulence: a field study in a *Sonneratia*-dominated mangrove forest, Vietnam. Cont. Shelf Res. 147, 114–127. https://doi.org/10.1016/j.csr.2017.06.002.

Phan, K.L., Stive, M.J.F., Zijlema, M., Truong, H.S., Aarninkhof, S.G.J., 2019. The effects of wave non-linearity on wave attenuation by vegetation. Coast. Eng. 147, 63–74. https://doi.org/10.1016/j.coastaleng.2019.01.004.

Quang Bao, T., 2011. Effect of mangrove forest structures on wave attenuation in coastal Vietnam. Oceanologia 53 (3), 807–818. https://doi.org/10.5697/oc.53-3.807.

Quartel, S., Kroon, A., Augustinus, P.G.E.F., Van Santen, P., Tri, N.H., 2007. Wave attenuation in coastal mangroves in the Red River Delta, Vietnam. J. Asian Earth Sci. 29 (4), 576–584. https://doi.org/10.1016/j.jseaes.2006.05.008.

Reef, R., Sayers, S., 2025. Wave attenuation by Australian temperate mangroves. J. Mar. Sci. Eng. 13 (2), 382. https://doi.org/10.3390/jmse13020382.

Samiksha, S.V., Vethamony, P., Bhaskaran, P.K., Pednekar, P., Jishad, M., James, R.A., 2019. Attenuation of wave energy due to mangrove vegetation off Mumbai, India. Energies 12 (22), 4286. https://doi.org/10.3390/en12224286.

Sánchez-Núñez, D.A., Mancera Pineda, J.E., Osorio, A.F., 2020. From local-to global-scale control factors of wave attenuation in mangrove environments and the role of indirect mangrove wave attenuation. Estuar. Coast. Shelf Sci. 245, 106926. https://doi.org/10.1016/j.ecss.2020.106926.

Suzuki, T., Hu, Z., Kumada, K., Phan, L.K., Zijlema, M., 2019. Non-hydrostatic modeling of drag, inertia and porous effects in wave propagation over dense vegetation fields. Coast. Eng. 149, 49–64. https://doi.org/10.1016/j.coastaleng.2019.03.011.

Temmerman, S., Horstman, E.M., Krauss, K.W., Mullarney, J.C., Pelckmans, I., Schoutens, K., 2023. Marshes and mangroves as nature-based coastal storm buffers. Annu. Rev. Mar. Sci. 15 (volume 15, 2023), 95–118. https://doi.org/10.1146/annurev-marine-040422-092951.

Tucker, M.J., Pitt, E.G., 2001. Waves in Ocean Engineering, 5. Elsevier Ocean Engineering Book Series, Elsevier, Amsterdam, p. 521.

Van Dijk, A.I.J.M., Beck, H.E., Boergens, E., Jeu, R.A.M. de, Dorigo, W.A., Edirisinghe, C., Forootan, E., Guo, E., Güntner, A., Hou, J., Mehrnegar, N., Mo, S., Preimesberger, W., Rahman, J., Rozas Larraondo, P., 2025. Global Water Monitor 2024, Summary Report. . Published by Global Water Monitor Consortium. www.globalwater.online.

Vanegas G, C.A., Osorio, A.F., Urrego, L.E., 2019. Wave dissipation across a *Rhizophora* mangrove patch on a Colombian Caribbean Island: an experimental approach. Ecol. Eng. 130, 271–281. https://doi.org/10.1016/j.ecoleng.2017.07.014.

Vo-Luong, P., Massel, S., 2008. Energy dissipation in non-uniform mangrove forests of arbitrary depth. J. Mar. Syst. 74 (1), 603–622. https://doi.org/10.1016/j.jmarsys.2008.05.004.

Wei, X., Mo, W., Xiong, L., Hu, X., Cheng, H., 2025. Field investigation of wave attenuation in a mangrove forest dominated by *Avicennia marina* (Forsk.) Viern. Plants 14 (1), 135. https://doi.org/10.3390/plants14010135.

Yoshikai, M., Nakamura, T., Bautista, D.M., Herrera, E.C., Baloloy, A., Suwa, R., Basina, R., Primavera-Tirol, Y.H., Blanco, A.C., Nadaoka, K., 2022. Field measurement and prediction of drag in a planted Rhizophora mangrove Forest. J. Geophys. Res. Oceans 127 (11). https://doi.org/10.1029/2021JC018320 e2021JC018320.

Zhang, X., Lin, P., Chen, X., 2022. Coastal protection by planted mangrove Forest during typhoon Mangkhut. J. Mar. Sci. Eng. 10 (9), 1288. https://doi.org/10.3390/jmse10091288.

Zhao, Z., Hu, Z., Bouma, T.J., 2025. Wave-Decay-Prediction-HU-Method. https://nioz.shinyapps.io/Wave-Decay-Prediction-HU-Method/.

Zhou, X., Dai, Z., Carniello, L., Long, C., Wang, R., Luo, J., Huang, Z., 2022. Linkage between mangrove wetland dynamics and wave attenuation during a storm–a case study of the Nanliu Delta, China. Mar. Geol. 454, 106946. https://doi.org/10.1016/j.margeo.2022.106946.